Journal of Materials Science and Chemical Engineering, 2025, 13(8), 15-27
https://www.scirp.org/journal/msce
ISSN Online: 2327-6053
ISSN Print: 2327-6045

Electrochemical Behavior of Photoactive Thin Solid Films of CdS/Poly (2-(2-Thienyl)furan) as an Inorganic/Organic Interface in Gel Electrolytes

Kasem K. Kasem, Joe Rousseau, Johnson Jr, Garrett Ray

School of Sciences, Indiana University Kokomo, Kokomo, USA
Email: kkasem@iu.edu

How to cite this paper: Kasem, K.K., Rousseau, J., Jr, J. and Ray, G. (2025) Electrochemical Behavior of Photoactive Thin Solid Films of CdS/Poly (2-(2-Thienyl)furan) as an Inorganic/Organic Interface in Gel Electrolytes. *Journal of Materials Science and Chemical Engineering*, **13**, 15-27.
https://doi.org/10.4236/msce.2025.138002

Received: July 16, 2025
Accepted: August 12, 2025
Published: August 15, 2025

Abstract

Inorganic/organic interface (I/O/I) Thin solid films made by incorporating cadmium sulfide (CdS) nanoparticles into poly (2-(2-thienyl)furan) (PTF) were subjected to optical and electrochemical investigation in a gel electrolyte. The studies indicate that CdS (n-type) and PTF (p-type) generate consistent photo response. UV-VIS absorption studies suggest that the formed CdS/PTF assembly demonstrates effective absorption across a broad range of photon energies, specifically between approximately 2.2 and 3.3 eV. The fact that PTFs are fluorescent, photoactive polymers promotes more efficient absorption of solar radiation energy and further utilization. Electrochemical studies in gel electrolytes indicate that the occlusion of CdS in PTF under illumination enhances their photoactivities. This is evidenced by larger photocurrents observed in both cathodic and anodic scans compared to those reported for pure PTF. It also indicates that CdS/PTF exhibits type II heterojunction behavior, which improves charge separation and decreases electron-hole recombination. Nyquist plots from electrochemical impedance spectroscopy (EIS) studies reveal a portion of the plot that is controlled by kinetics at high frequencies. Conversely, at low frequencies, Warburg diffusion control is observed. The studied assemblies exhibited stability and resistance to photodegradation, as demonstrated by the regeneration of the same photo response after an extended period of experimentation.

Keywords

Photo-Electrochemistry, Inorganic-Organic, Heterojunction, Gel Electrolyte

1. Introduction

The creation of hybrid materials with a large surface area interface can be achieved by leveraging the diffuse nature of the HOMO and LUMO levels in organic semiconductors. This diffusive characteristic enables effective coupling with inorganic semiconductors, broadening the light absorption range. This advancement could facilitate the development of functional hybrid materials by sensitizing large bandgap inorganic semiconductors. The ideal photoactive hybrid interface must ensure that its organic and inorganic components maintain compatibility and function effectively together, with intangible stability toward photodecomposition.

Assemblies include semiconductors in the form of thin film electrodes or colloidal systems that might be used in solid or liquid photovoltaic cells were studied [1]-[6]. Additional assemblies, such as metal chalcogenides modified with polyaniline, polypyrene, or other organic semiconductors, were studied [7]-[9] to name but a few. However, these studies reported low conversion efficiencies. Metal, chalcogenide, and oxide semiconductors absorb solar radiation matching their band gaps. Their surfaces can be modified to broaden the absorption spectrum with agents that absorb ultraviolet (UV) light. Many conjugated organic semiconductors can absorb UV radiation and re-emit it for longer. Modified CdS with poly Ru vinyl bipyridine, was investigated [10] [11] in the form of thin solid films in aqueous electrolytes.

Assemblies involving cadmium chalcogenides such as CdSe, CdS with polythiophenes, and other photoactive organic compounds were investigated [12]-[15]. Further, carbon nanotubes in interface with CoS_2 [16] and N-based organic polymers interfaced with ZnS [17] or organic/metal assemblies [18] were investigated. Using these interfaces to build organic electronics or hybrid organic solar cells [19] has been achieved.

The electrolyte component in the photoactive interface plays a crucial role in the assembly of functional hybrid materials. The effectiveness of a photoactive interface is influenced by the type of electrolyte used. This is essential for improving the kinetics of oxygen (O_2) evolution on the surface of the photoanode during photolysis in aqueous electrolytes. Certain ions in aqueous solutions can deplete photo-generated holes and inhibit oxygen evolution. Investigating the same photoactive interface in various electrolytes, like gel electrolytes, can help identify optimal conditions for maximizing photochemical performance and ensuring long-term stability.

Polymer gel electrolytes provide an alternative to liquid electrolytes, reducing erosion in photoactive film assemblies of photoelectrochemical cell devices. One type of these gel electrolytes is thermoplastic gel electrolytes (TPGE). Multiple studies have focused on the fabrication, operating principles, and current status of dye-sensitized solar cells (DSSCs) and batteries utilizing polymer electrolytes. [20] [21]. We chose the I^-/I_3^- redox-active material for the proposed TPGE due to its advantageous properties, such as good solubility, low light absorption, suitable

redox potential, fast dye generation, and minimal recombination with certain inorganic semiconductors [22]-[25].

Sulfur is essential for the photoactivation of sulfur-containing compounds, particularly in biological systems, as it participates in redox reactions and helps form crucial compounds. In ionic sulfur compounds, sulfur vacancies can modify the electronic structure and serve as electron reservoirs, enhancing adsorption and activation sites. Sulfur in organic compounds serves as a semiconductor photocatalyst, facilitating carbon-sulfur bond formation and the generation of reactive species for environmental remediation.

In this study, we investigated the electrochemical properties of amorphous n-type CdS nanoparticles embedded within a p-type poly (2-(2-thienyl)furan) (PTF). The objective was to understand how the occlusion of CdS (ionic Sulfur) within PTF (covalent sulfur) affects photoelectrochemical outcomes in gel electrolytes. Additionally, we explored whether the presence of CdS in the PTF network alters the π-bonding interactions, which could influence the overall interaction between CdS and the host polymer.

2. Experimental

2.1. Reagents

The monomer (2-(2-thienyl)furan) (TF), amorphous nanoparticles of cadmium sulfide (CdS), and Lithium perchlorate ($LiClO_4$), were of analytical grade. Unless otherwise stated.

2.2. Preparations

Inorganic/organic interface (IOI) assemblies CdS/PTF thin films were prepared using the occlusion method as previously described [26]. The ratio of CdS to monomer solution was 20 mg/ml. The thickness of the prepared films was measured and calibrated using spectroscopic reflectance measurements controlled by the corresponding software. The thickness of the electropolymerized films ranged from 900 to 1100 nm.

Thermoplastic gel electrolyte (TPGE) was prepared following the published procedure [27]. Briefly, 0.65 M KI and 0.065 M I_2 were dissolved in 10 mL polycarbonate (PC), and then 8.5 g of PEG (M-20000) was added to the mixture. The mixture was heated at 100˚C under continuous stirring for ca. 12 h in a flask under an inert atmosphere. The mixture was hydrothermally treated at 180˚C for 14 h in a Teflon autoclave.

2.3. Instrumentation

A conventional three-electrode cell consisting of a Platinum (Pt) wire as a counter electrode, an Ag/AgCl reference electrode, and FTO with a surface area of 2.0 cm^2 was used as the working electrode for electrochemical preparation of the photoactive polymer. Photoelectrochemical studies of the thin solid films were performed using the experimental setup as described in previous work [27]. Plati-

nized FTO is used as both the reference and counter electrode due to its high conductivity in gel electrolytes and improved light transparency. A Solartron 2101A was used for the electrochemical impedance spectroscopy (EIS) studies, conducted in a frequency range of 0.01 to 100 kHz. A BAS 100W electrochemical analyzer (Bioanalytical Co., IN) was used to perform the electrochemical studies. Optical parameters were calculated based on the steady-state reflectance spectra, measured by a Shimadzu UV-2101PC spectrophotometer. An Olympus BX-FL Irradiation was performed using a 300-watt xenon lamp solar simulator (Newport, NJ) with an IR filter. All measurements were performed at 298 K. Unless otherwise stated, all potentials were measured against platinized FTO (0.597 vs. SHE).

3. Results and Discussions

3.1. Absorption Spectra Studies

The light absorption of the assembly consisting of CdS/PTF has been examined. The results are presented in **Figure 1**. **Figure 1(A)**, trace 1 shows a broader absorption peak for CdS/PTF, while trace 2 shows multiple absorption peaks for PTF. This is consistent with previous studies and reflects the presence of several oligomers with different HOMO/LUMO gaps (26). **Figure 1(A)**, trace 1, also shows that the assembly made by occlusion of CdS in PTF shows effective absorption of a wide range of photon energies between ≈2.2 and ≈3.3 eV. **Figure 1(B)** and **Figure 1(C)** show Tauc plots obtained to analyze the absorption data in **Figure 1(A)**. These plots show that both direct and indirect band gaps coexist due to the presence of oligomers.

3.2. Emission Spectra Studies on PTF

In PTF, increasing side-chain bulk restricts rotation, often enhancing fluorescence by increasing rigidity and limiting conformational disorder. The thin solid film of PTF possesses the quality of structural rigidity, π-conjugated systems, that restrict these motions, channeling more energy into radiative decay (fluorescence), leading to enhanced fluorescence intensity. Further, the fact that the film shows a good response to emission indicates that this film's rigid, planar backbones promote better conjugation, which lowers the bandgap and increases fluorescence efficiency.

Thin films of PTF were excited with white polychromatic light, and the emitted radiation was subsequently measured. The results are shown in **Figure 2**, which shows the absorption and fluorescence emission spectra of PTF. The observation that PTF emits fluorescence at longer wavelengths confirms the formation of a photoactive assembly. This assembly effectively utilizes absorbed photons, emitting them at longer wavelengths, which are then reabsorbed again. This would increase the range of visible radiation when the absorption intensity is low at short wavelengths. As the assembly contains a variety of polymers and oligomers, the emitted radiation at (ca $\lambda = 450$, **Figure 2** trace b) can be absorbed by short-chain

oligomers that coexist in the studied assembly and possess a larger band gap. On the other hand, the emitted radiation at (ca $\lambda > 550$, Figure trace b broader peak) can be absorbed by longer-chain polymers, which possess a smaller band gap than shorter-chain oligomers. Figure 2 provides strong evidence that PTFs are fluorescent photoactive polymers. Their significance lies in their potential contributions to advanced materials science and technology, including applications in medical diagnostics, sensors, and organic light-emitting diodes (OLEDs). Their capability to respond to light not only enhances the functionality of devices but also promotes more efficient energy usage. The results shown in Figure 2 remained consistent over months, indicating their excellent photostability.

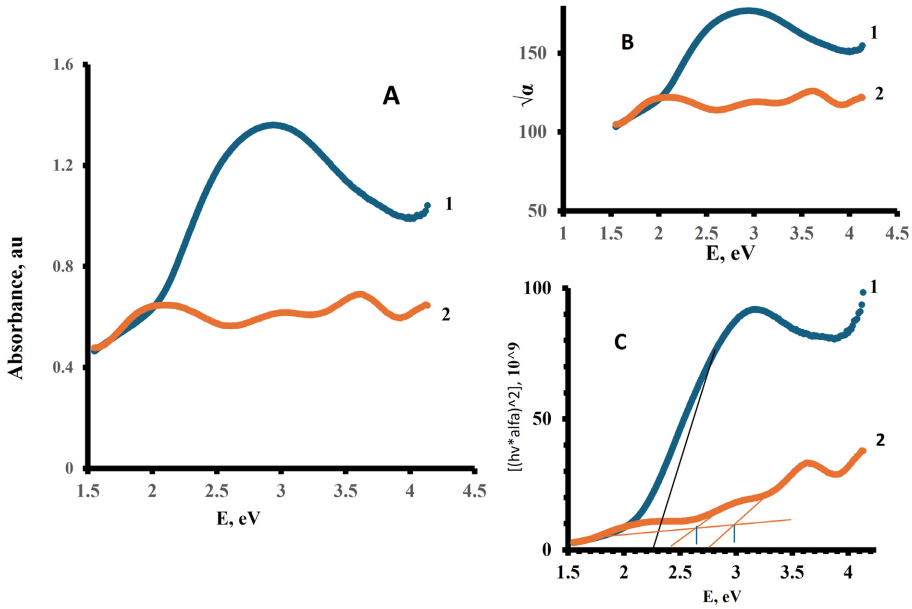

Figure 1. A) Absorption spectra for 1-/CdS/PTF, 2-PTF, B) $\sqrt{a}$ vs. Photon Energy, eV, and C) $(a)^2$ vs Photon energy, eV.

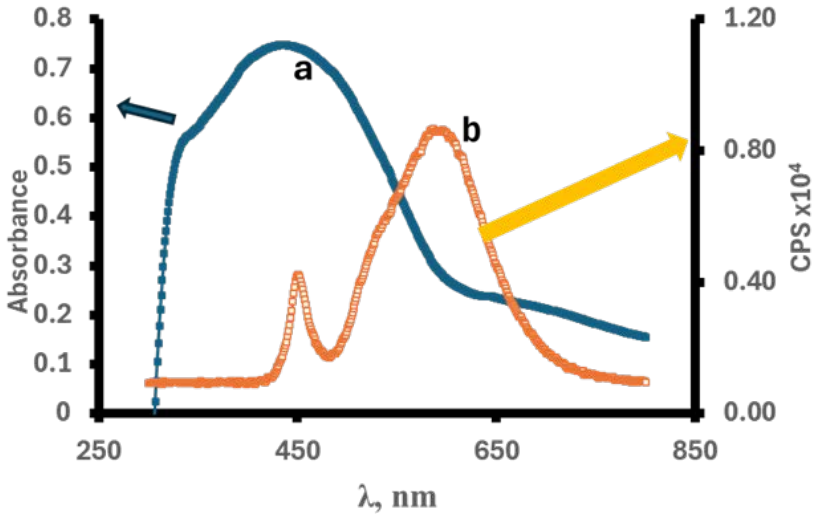

Figure 2. Absorption-Fluorescence of a thin solid film of PTF, Excitation with white LED, (a) Absorption spectra, (b) Fluorescence spectra.

3.3. Photoelectrochemical (PEC) Studies

All electrochemical studies conducted in gel electrolytes occurred in the electrochemical cells described in [26] [27], where the modified FTO with either inorganic or organic PTF serves as the working electrode, thermoplastic KI/I_3^- -gel functions as the electrolyte, and platinized FTO (Pt/FTO) serves as both the counter and reference electrode. In-situ monomer/polymer transition studies are performed when TF is involved in any process. The studies were conducted in the dark and under illumination, with a scan rate of 0.10 V/s unless otherwise stated. Some of the CVs are shown in **Figure 3** and **Figure 4**. A closer examination of **Figure 3(A)** reveals that there is an increase in photocurrent for PTF/FTO during both anodic and cathodic scans upon illumination. Trace 1 in **Figure 3(A)** demonstrates the behavior of CdS/TF in the dark. In contrast, trace 2 shows a significantly higher photocurrent for CdS/TF when illuminated, which can be attributed to the presence of CdS. Trace 3 indicates an even greater photocurrent generated by the illuminated assembly of CdS/PTF. This substantial increase is a combined effect of both CdS and PTF. CdS enhances the process of charge separation, resulting in an improved photocurrent.

Figure 3(B) illustrates the chronoamperometric studies conducted on CdS/PTF at a voltage of -1.2 V. The results reveal a gradual increase in photocurrent when exposed to light, followed by a gradual decrease in current when returning to darkness. This behavior suggests that there is no evidence of hole accumulation or electron back scattering, which is typically observed in undoped PTF [26]. Furthermore, **Figure 3(B)** indicates no sudden drop in the measured current when the light is turned off. The current generated without illumination is referred to as dark current. This phenomenon is attributed to the random generation of electron-hole pairs within the depletion region at the CdS/PTF interface [28] [29].

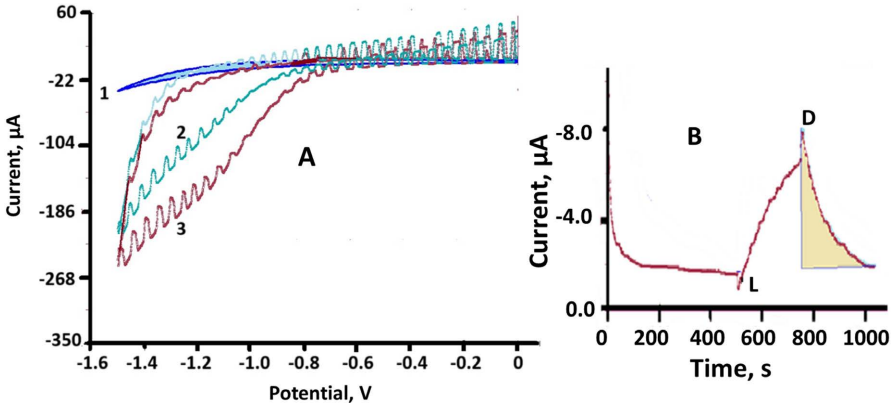

Figure 3. (A) I vs E at scan rate 0.1 V.s-1 for PTF/CdS/Gel electrolyte/(Pt-FTO)/Gel electrolyte: 1-TF/CdS (D), 2-TF/CdS (L), and 3-PTF/CdS(L), (B) Chronoamperometric studies at -1.2 V vs Pt-FTO. D = dark. And L = Light, D = dark. And L = Light.

Figure 4(A) illustrates an increase in photocurrent for PTF/FTO during both anodic and cathodic scans when exposed to illumination. Trace 1 in **Figure 4(A)** represents the behavior of CdS/PTF in the dark, while Trace 2 demonstrates the

behavior of CdS/PTF under illumination. The anodic scan concentrated on the potential range of 0.2 to 2.0 V to examine the behavior of CdS/PTF under oxidation conditions. The results are shown in Figure 4(B). This figure illustrates the chronoamperometric studies conducted on CdS/PTF at a voltage of 1.2 V. Upon the onset of illumination, there is a sharp increase in current, which is followed by a rapid decline for a brief period, after which the current begins to rise again until it reaches a steady state. In contrast, the current experiences a sudden drop under dark conditions, followed by a gradual decay (Shaded area). These observations may be attributed to capacitive effects or an imbalance between the rapid generation and the slower transport of charges, possibly indicating a charge redistribution or back-diffusion process.

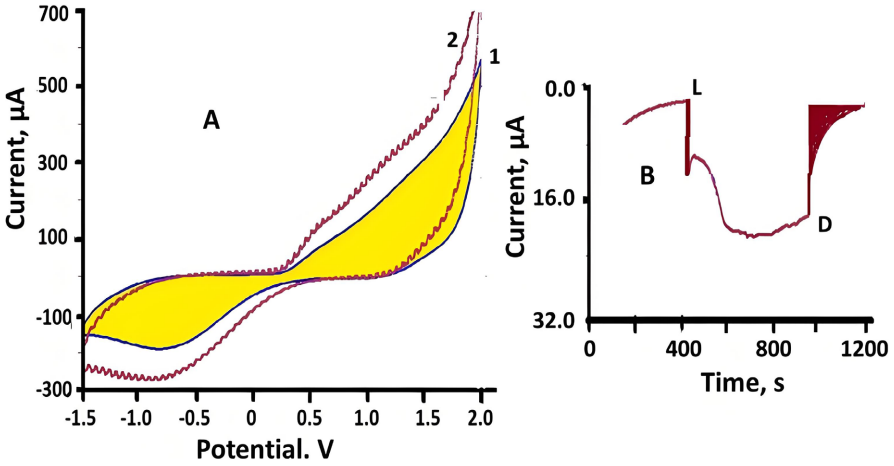

Figure 4. (A) I vs E at scan rate 0.1 V.s-1 for PTF/CdS/Gel electrolyte/(Pt-FTO)/Gel electrolyte: 1-PTF/CdS (D), and 2-PTF/CdS (L), (B) Chronoamperometric studies at 1.2 V vs Pt-FTO. D = dark. And L = Light.

Table 1. Photocurrent (I_P) generation by the assembly FTO/PTF and FTO/CdS/PTF.

Assembly	I_P, µA at −1.2 V	I_P, µA at +1.2 V
FTO/PTF	120.0	80.0
FTO/CdS/PTF	166.0	120.0

The data listed in Table 1, generated from Figure 3 and Figure 4 and compared with the CV behavior of PTF alone in the same gel electrolytes [26], show that occlusion of CdS into PTF enhanced the photo activities, evidenced by the larger photocurrent in both cathodic and anodic scans than that reported for pure PTF. A closer look at the assembly of the CdS/PTF interface, the electron affinity (EA) of CdS is approximately ≈ 4.2 eV, while that of PTF is ≈ 3.4 eV. This results in a conduction band offset of about 0.8 eV, facilitating electron confinement in CdS and promoting hole transfer into PTF. Consequently, CdS/PTF exhibits type II heterojunction behavior, which enhances charge separation and reduces the likelihood of electron-hole recombination. This phenomenon helps explain why the

photocurrent generated from the CdS/PTF combination is greater than that produced by either CdS or PTF alone.

4. Electrochemical Impedance Spectroscopy (EIS) Studies

The Electrochemical Impedance Spectroscopy (EIS) of the studied assemblies, FTO/PTF and FTO/CdS/PTF, in gel electrolyte, was conducted at frequencies ranging from 10^5 to 10^-1 Hz. The Nyquist plots and other dielectric properties generated from the assemblies on the FTO substrate, both in the dark and under illumination, are presented in **Figure 5** and **Figure 6**. **Figure 5** demonstrates that illuminating the host polymer (PTF) decreases the imaginary component of the impedance across all applied frequencies (**Figure 5(A)** trace 1). Furthermore, it indicates that the assemblies studied exhibit a porous film structure that does not reach a state of charge saturation at very low frequencies. Additionally, a distinct portion of the Nyquist plot reveals the Warburg zone [30].

Figure 5(B) shows a plot of log σ (conductivity) versus log ω (frequency). Under illumination, the AC conductivity of FTO/PTF (represented by trace 1 in **Figure 5(B)**) increases with rising frequency for the studied assemblies. However, it remains lower than the conductivity measured in the dark condition, which is up to approximately 100 Hz. Beyond this frequency, the AC conductivity under illumination surpasses the levels observed in the dark. After around 10 kHz, there is a slight increase in conductivity. This behavior was observed and explained on the basis that at high frequencies, the increased capacitive reactance of the studied assembly is a major factor in the observed conductivity decrease [31].

Figure 6(A) displays a Nyquist plot for FTO/CdS under illumination (trace 1) and in the dark (trace 2). In a dark, clear semicircle that always indicates the presence of kinetic control at high and low frequencies. On the other hand, **Figure 6(B)** indicates that in the dark, the conductivity of the FTO/ CdS is higher than that measured under illumination.

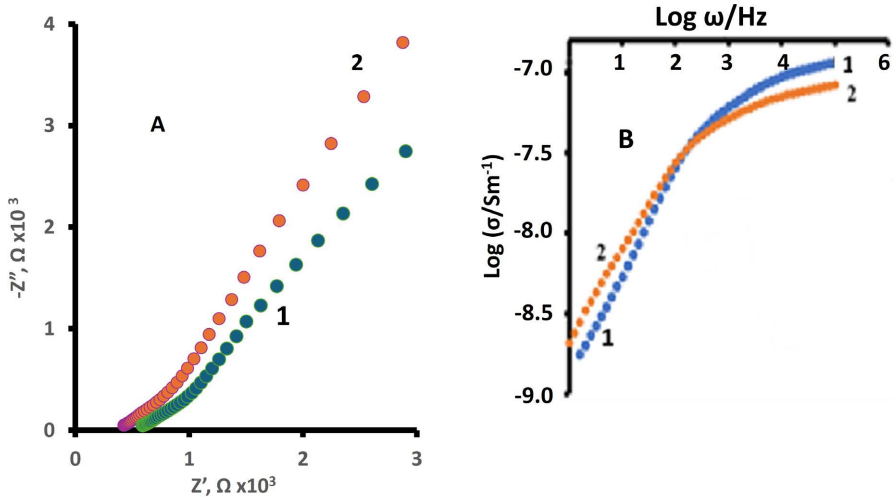

Figure 5. (**A**) Nyquist plot for FTO/PTF, at 0.0 V, (**B**) Log electrical conductivity σ vs. Log Frequency ω, for FTO/PTF, at 0.0 V, 1-Light, and 2-Dark.

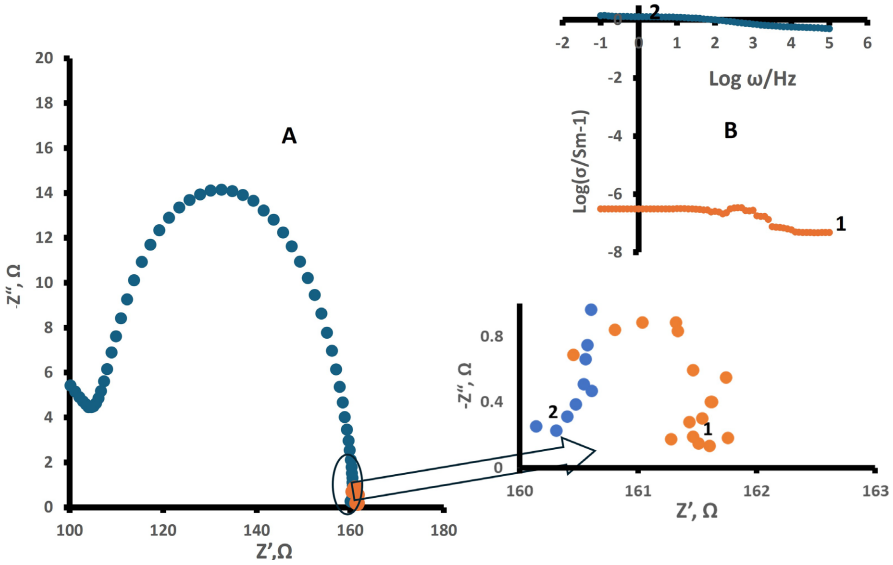

Figure 6. (A) Nyquist plot for FTO/CdS, at 0.0 V vs platinized FTO (**B**) Log electrical conductivity σ vs. Log Frequency ω, for FTO/CdS, at 0.0 V, 1-Light, and 2-Dark.

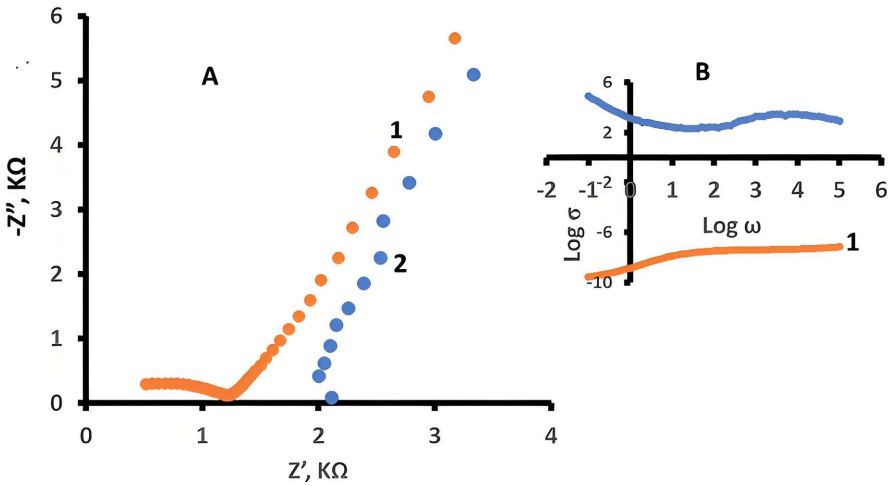

Figure 7. (A) Nyquist plot for FTO/CdS/PTF, at 0.0 V, (B) Log electrical conductivity σ vs. Log Frequency ω, for FTO/CdS/PTF, at 0.0 V, 1-Light, and 2-Dark.

Figure 7(A) shows a significant effect of occluding CdS in PTF. Under illumination of the CdS/PTF, both the observed imaginary and real impedance values were lower than those observed in the dark. In Figure 7(A), race 1, it is also evident that there is a noticeable portion of the plot governed by kinetic control at high frequencies. In contrast, at low frequencies, Warburg diffusion control was observed. Figure 7(B) indicates that in the dark, the conductivity of the CdS/PTF assembly is higher than that measured under illumination.

The plots of log σ vs. log ω (Figure 6(B) and Figure 7(B)) at 0.0 V vs. Platinized FTO show that CdS—either alone or in combination with PTF—exhibits greater conductivity in the dark than under illumination. This suggests that CdS is the primary factor contributing to this unusual behavior.

This phenomenon may be due to a possible photo-desorption of surface-ad-

sorbed oxygen [32] when illuminated. When O_2 is adsorbed onto the CdS surface, it captures electrons and forms O_2^- species. Under illumination, photons generate electron-hole pairs. The holes migrate to the surface, neutralizing O_2^-, which leads to the desorption of oxygen. One might expect this to decrease conductivity, as the desorption of O_2 may expose surface trap states or increase recombination, ultimately reducing effective carrier mobility and lowering conductivity. In the presence of PTF, surface trap states were further exposed by the polymer units. Another possibility involves the photo-charging effects in the electrochemical setup using FTO/CdS or FTO/CdS/PTF in contact with a gel electrolyte containing the I_3^-/I_2 /I_2 redox system. When illuminated, electrons may transfer from CdS to the redox species in the solution. This transfer of electrons depletes CdS, resulting in a reduction of its conductivity.

5. Conclusion

The enhanced photoactivity of the CdS/PTF assembly, compared to that of PTF alone, as evidenced by the larger observed photocurrent (**Table 1**), suggests that CdS plays a crucial role in improving charge separation and, consequently, charge transfer. The improved photoelectrochemical behavior is attributed to the formation of a hybrid organic/inorganic interface between CdS and PTF. This enhancement is likely achieved through better charge separation, transfer, and optimized band alignments between the materials, making these assemblies potentially useful in photoelectrochemical devices.

Declaration of Competing Interest

The authors declare that they have no known competing financial interests or personal relationships that could have appeared to influence the work reported in this paper.

Acknowledgement

The authors acknowledge the support for this work from Indiana University Kokomo.

Conflicts of Interest

The authors declare no conflicts of interest regarding the publication of this paper.

References

[1] Heera, T.R. and Cindrella, L. (2011) PbS/CoS-Pani Composite Semiconductor Films. *Materials Science in Semiconductor Processing*, **14**, 151-156. https://doi.org/10.1016/j.mssp.2011.02.002

[2] Mahesh, A. (2011) Photovoltaic Performance of ZnO Nanosheets Solar Cell Sensitized with β-Substituted Porphyrin. *Journal of Nanomaterials*, **2011**, Article ID: 301873. https://doi.org/10.1155/2011/301873

[3] Hahlin, M., Johansson, E.M.J., Plogmaker, S., Odelius, M., Hagberg, D.P., Sun, L., *et*

al. (2010) Electronic and Molecular Structures of Organic Dye/TiO_2 Interfaces for Solar Cell Applications: A Core Level Photoelectron Spectroscopy Study. *Physical Chemistry Chemical Physics*, **12**, 1507-1517. https://doi.org/10.1039/b913548k

[4] Blumstengel, S., Koch, N., Sadofev, S., Schäfer, P., Glowatzki, H., Johnson, R.L., *et al.* (2008) Room Temperature Ferromagnetism in ZnO Films due to Defects. *Applied Physics Letters*, **92**, 193303-193306.

[5] Adams, D.M., Brus, L., Chidsey, C.E.D., Creager, S., Creutz, C., Kagan, C.R., *et al.* (2003) Charge Transfer on the Nanoscale: Current Status. *The Journal of Physical Chemistry B*, **107**, 6668-6697. https://doi.org/10.1021/jp0268462

[6] Thomas, K.G. and Kamat, P.V. (2003) Chromophore-Functionalized Gold Nanoparticles. *Accounts of Chemical Research*, **36**, 888-898. https://doi.org/10.1021/ar030030h

[7] Kasem, K.K., Menges, S. and Jones, S. (2009) Photoelectrochemical Studies on Poly[1-(2-Aminophenyl)Pyrrole]—Creation of a Photoactive Inorganic-Organic Semiconductor Interface (IOI). *Canadian Journal of Chemistry*, **87**, 1109-1116. https://doi.org/10.1139/v09-079

[8] Grätzel, M. (2001) Photoelectrochemical Cells. *Nature*, **414**, 338-344. https://doi.org/10.1038/35104607

[9] Zhang, Q., Wu, T., Bu, X., Tran, T. and Feng, P. (2008) Ion Pair Charge-Transfer Salts Based on Metal Chalcogenide Clusters and Methyl Viologen Cations. *Chemistry of Materials*, **20**, 4170-4172. https://doi.org/10.1021/cm800904d

[10] Kasem, K.K. (1999) Photo-Electrochemistry at Polymer/Semiconductor Interface Characterization of Surface Modified CdS-Based Photovoltaic Cells. *Journal of Materials Science*, **34**, 5237-5242. https://doi.org/10.1023/a:1004772231981

[11] Kasem, K.K. (1999) Photoelectrochemical Studies on Stationary Surface Modified CdSe Electrodes. *Materials Science and Engineering: B*, **65**, 127-134. https://doi.org/10.1016/s0921-5107(99)00218-4

[12] de Freitas, J.N., Grova, I.R., Akcelrud, L.C., Arici, E., Sariciftci, N.S. and Nogueira, A.F. (2010) The Effects of CdSe Incorporation into Bulk Heterojunction Solar Cells. *Journal of Materials Chemistry*, **20**, 4845-4853. https://doi.org/10.1039/c0jm00191k

[13] Ananthakumar, S., Ramkumar, J. and Moorthy Babu, S. (2014) Synthesis of Thiol Modified CdSe Nanoparticles/P3HT Blends for Hybrid Solar Cell Structures. *Materials Science in Semiconductor Processing*, **22**, 44-49. https://doi.org/10.1016/j.mssp.2014.02.008

[14] Otero, M., Dittrich, T., Rappich, J., Heredia, D.A., Fungo, F., Durantini, E., *et al.* (2015) Photoinduced Charge Separation in Organic-Inorganic Hybrid System: C_{60}-Containing Electropolymer/CdSe-Quantum Dots. *Electrochimica Acta*, **173**, 316-322. https://doi.org/10.1016/j.electacta.2015.05.029

[15] Shoyiga, H.O., Akpasi, S.O., Akpan, J., Amune, U.O. and Kiambi, S.L. (2024) Novel Photoactive Material and Fabrication Techniques for Solar Cells Application: Nanocellulose-Based Graphene Oxide CdS Composite. *Clean Energy*, **8**, 189-216. https://doi.org/10.1093/ce/zkae010

[16] Liu, T., Mai, X., Chen, H., Ren, J., Liu, Z., Li, Y., *et al.* (2018) Carbon Nanotube Aerogel-CoS_2 Hybrid Catalytic Counter Electrodes for Enhanced Photovoltaic Performance Dye-Sensitized Solar Cells. *Nanoscale*, **10**, 4194-4201. https://doi.org/10.1039/c7nr09260a

[17] Wei, H., Yan, X., Li, Y., Wu, S., Wang, A., Wei, S., *et al.* (2012) Hybrid Electrochromic Fluorescent Poly(DNTD)/CdSe@ZnS Composite Films. *The Journal of Physical Chem-*

istry C, **116**, 4500-4510. https://doi.org/10.1021/jp2117906

[18] Chen, Y., Tamblyn, I. and Quek, S.Y. (2017) Energy Level Alignment at Hybridized Organic-Metal Interfaces: The Role of Many-Electron Effects. *The Journal of Physical Chemistry C*, **121**, 13125-13134. https://doi.org/10.1021/acs.jpcc.7b00715

[19] Zhong, Y., Tada, A., Geng, Y., Wei, Q., Hashimoto, K. and Tajima, K. (2013) Donor/Acceptor Interface Modifications in Organic Solar Cells. *Journal of Photopolymer Science and Technology*, **26**, 181-184. https://doi.org/10.2494/photopolymer.26.181

[20] Singh, R., Polu, A.R., Bhattacharya, B., Rhee, H., Varlikli, C. and Singh, P.K. (2016) Perspectives for Solid Biopolymer Electrolytes in Dye Sensitized Solar Cell and Battery Application. *Renewable and Sustainable Energy Reviews*, **65**, 1098-1117. https://doi.org/10.1016/j.rser.2016.06.026

[21] Harvey, P.E., MacCallum, J.R. and Vincent, C.A. (1989) Polymer Electrolyte Reviews. Elsevier.

[22] Kato, Y., Hori, S., Saito, T., Suzuki, K., Hirayama, M., Mitsui, A., *et al.* (2016) High-Power All-Solid-State Batteries Using Sulfide Superionic Conductors. *Nature Energy*, **1**, Article No. 16030. https://doi.org/10.1038/nenergy.2016.30

[23] Xue, Z., He, D. and Xie, X. (2015) Poly(Ethylene Oxide)-Based Electrolytes for Lithium-Ion Batteries. *Journal of Materials Chemistry A*, **3**, 19218-19253. https://doi.org/10.1039/c5ta03471j

[24] Haque, S.A., Palomares, E., Upadhyaya, H.M., Otley, L., Potter, R.J., Holmes, A.B., *et al.* (2003) Flexible Dye Sensitised Nanocrystalline Semiconductor Solar Cells. *Chemical Communications*, No. 24, 3008-3009. https://doi.org/10.1039/b308529e

[25] Xiao, Q.C., Liu, H.Y., Xia, Q.L., Xiao, Q.Z., Lei, G.T. and Li, Z.H. (2014) A Nanocomposite Polymer Electrolyte with High-Temperature Stability for Rechargeable Lithium Batteries. *Arabian Journal for Science and Engineering*, **39**, 6651-6657. https://doi.org/10.1007/s13369-014-1180-x

[26] Kasem, K., Masuda, H. and Mendez Rodriguez, A. (2024) Tracking the Photoactivity at the Interface of SiC/Poly 2(2-Thienyl) Furan Thin Solid Film in Polymer Gel Electrolytes. *Journal of Electrochemical Science and Engineering*, **14**, 671-684. https://doi.org/10.5599/jese.2401

[27] Kasem, K.K. (2021) Long-term Activity of Thermoplastic Gel Electrolyte in a Photo-Electrochemical Assembly Involving Poly Bithiophene (PBTh) as Photoactive Working Electrode. *Journal of Materials Science and Chemical Engineering*, **9**, 1-11. https://doi.org/10.4236/msce.2021.96001

[28] Wu, J.H., Hao, S.C., Lan, Z., Lin, J.M., Huang, M.L., Huang, Y.F., *et al.* (2007) A Thermoplastic Gel Electrolyte for Stable Quasi-Solid-State Dye-Sensitized Solar Cells. *Advanced Functional Materials*, **17**, 2645-2652. https://doi.org/10.1002/adfm.200600621

[29] Kasem, K.K. and Russeau, J. (2024) Electrochemical Studies on Photoactive Thin Solid Films of Poly (2-(2-Thienyl) Furan) Occluded with a G-C_3N_4/SiC Mixture in Gel Electrolyte. *Journal of Materials Science and Chemical Engineering*, **12**, 54-66. https://doi.org/10.4236/msce.2024.1212004

[30] Go, E., Jin, H., Yoon, S., Park, S., Park, S.H., Yu, H., *et al.* (2022) Unraveling the Origin of Dark Current in Organic Bulk Heterojunction Photodiodes for Achieving High Near-Infrared Detectivity. *ACS Photonics*, **9**, 2056-2065. https://doi.org/10.1021/acsphotonics.2c00193

[31] Li, C., Bando, Y., Liao, M., Koide, Y. and Golberg, D. (2010) Visible-Blind Deep-

Ultraviolet Schottky Photodetector with a Photocurrent Gain Based on Individual Zn_2GeO_4 Nanowire. *Applied Physics Letters*, **97**, Article ID: 161102. https://doi.org/10.1063/1.3491212

[32] Chen, J., Unjaroen, D., Stepanovic, S., van Dam, A., Gruden, M. and Browne, W.R. (2018) Selective Photo-Induced Oxidation with O_2 of a Non-Heme Iron(III) Complex to a Bis(Imine-Pyridyl)Iron(II) Complex. *Inorganic Chemistry*, **57**, 4510-4515. https://doi.org/10.1021/acs.inorgchem.8b00187